EBioMedicine
Published by THE LANCET

Blockade of miR-3614 maturation by IGF2BP3 increases TRIM25 expression and promotes breast cancer cell proliferation

Zhenzhen Wang [a,b,1], Dongdong Tong [b,1], Cong Han [b], Zhenghao Zhao [c], Xiaofei Wang [b], Ting Jiang [b], Qian Li [b], Siyuan Liu [b], Lin Chen [d], Yanke Chen [b,**], Ang Li [a,*], Chen Huang [a,b,*]

[a] Key Laboratory of Shaanxi Province for Craniofacial Precision Medicine Research, College of Stomatology, Xi'an Jiaotong University, Xi'an 710004, China
[b] Key Laboratory of Environment and Genes Related to Diseases, Ministry of Education of China, Xi'an Jiaotong University, Xi'an 710061, China
[c] The ART Center, Northwest women's and Children's Hospital, Xi'an, China
[d] The Pathology Department, Shanxi Provincial People's Hospital, Xi'an, China

ARTICLE INFO

ABSTRACT

Background: The cross-talk between RNA binding proteins (RBPs) and microRNAs (miRNAs) in the regulation of gene expression is a complex process. Here, we describe a new mode of regulation of TRIM25 expression mediated by an antagonistic interplay between IGF2BP3 and miR-3614-3p.
Methods: The expression level of TRIM25, IGF2BP3, pri-miR-3614 and miR-3614-3p in breast cancer (BC) tissues, non-tumor tissues and BC cell lines were detected by qRT-PCR, Western blot and Immunohistochemistry (IHC). Binding of miR-3614-3p and IGF2BP3 to TRIM25 RNA was verified using luciferase activation assays, RNA immunoprecipitation (RIP) and biotin pull-down assays. In vitro and in vivo loss- and gain-of-function studies were performed to reveal the effects and related mechanism of IGF2BP3-miR-3614-3p-TRIM25 axis in in breast cancer cells proliferation.
Findings: We found that an intragenic miRNA-3614-3p inhibits the expression of its host gene TRIM25 by binding to its 3′- untranslated region (UTR). Interestingly, IGF2BP3 can competitively occupy this binding site and inhibit miRNA-3614 maturation, thereby protecting TRIM25 mRNA from miR-3614-mediated degradation. The overexpression of miR-3614-3p dramatically inhibited breast cancer cell growth through the downregulation of TRIM25. Furthermore, the silencing of IGF2BP3 reduced TRIM25 expression, suppressed cell proliferation, and exhibited a synergistic effect with miR-3614-3p overexpression.
Interpretation: Collectively, these results demonstrate that control of TRIM25 RNA by an interplay between IGF2BP3 and miR-3614-3p represents a mechanism for breast cancer cell proliferation.
Fund: The scientific research and sharing platform construction project of Shaanxi Province, Opening Project of Key Laboratory of Shaanxi Province for Craniofacial Precision Medicine Research, China Postdoctoral Science Foundation and The National Natural Science Foundation of China.

1. Introduction

Post-transcriptional gene regulation (PTGR) involves complex processes that modulate the transcription, transport, maturation, translation, and stability of coding and non-coding RNAs [1,2]. Post-transcriptional modifications can have profound effects on gene expression; RNA-binding proteins (RBPs) and microRNAs (miRNAs) are potent post-transcriptional regulators of gene expression. Most commonly, they converge at the 3′-UTRs of mRNAs and affect the stability and translation of the transcripts [3,4].

The RBP family is composed of approximately 800 proteins with conserved domains. RBPs bind to double- or single-stranded RNA and regulate RNA fate from synthesis to decay [5]. The insulin-like growth factor 2 mRNA binding protein 3 (IGF2BP3) stabilizes and facilitates the translation of numerous target mRNAs [6]. IGF2BP3 belongs to a conserved family of RBPs. Previous studies have demonstrated that the binding of IGF2BP3 to target mRNAs stabilizes the mRNA, thereby preventing its decay [7]. Interestingly, one putative mechanism suggests that IGF2BP3 and miRNAs converge on the 3′-UTRs of target transcripts to upregulate or downregulate genes that are associated

with malignancy [8]. However, whether and how IGF2BP3 is involved in the miRNA-mediated gene silencing to regulate translation in cancer cells remains to be determined.

MiRNAs are synthesized as longer transcripts primary (Pri)miRNAs that are processed by the nuclear RNase III Drosha into 70-nt, hairpin precursor miRNAs (Pre)miRNAs. These are further processed in the cytoplasm by RNase III, giving rise to mature miRNAs that assemble with members of the Argonaute (Ago) protein family to form the RNA-induced silencing complex (RISC) [9–11]. The biogenesis of miRNAs occurs at two locations. The intergenic miRNAs are derived from noncoding regions between genes and are transcribed by unidentified promoters [11]. Most miRNAs are recognized as intergenic miRNA. A minority of miRNAs are derived from noncoding introns or the 5′-UTRs and the 3′-UTRs of host genes. These miRNAs are termed intronic or intragenic miRNAs [12], and have been reported to play various roles in host gene regulation [13]. Although several studies on intronic miRNAs have been conducted, whether intronic miRNAs can exhibit inhibitory effects on host genes remains to be determined.

In this study, we report that the intragenic mature miR-3614 can silence the expression of its host gene, tripartite motif-containing 25 (_TRIM25_), which is also regulated by IGF2BP3. Several studies have shown that IGF2BP3 is involved in the stabilization of mRNAs encoding IGF2, HMGA2, CD44, and PDPN [14–16]. However, little is known about the role of IGF2BP3 in modulating the cytoplasmic fate of TRIM25 mRNA. TRIM25, an estrogen-responsive RING finger protein (Efp), is mainly expressed in estrogen target tissues, such as mammary glands and the uterus [17]. Accumulating evidence demonstrates that in MCF-7 BC cells, TRIM25 mediates degradation of 14-3-3σ, a negative cell cycle regulator. Loss of _TRIM25_ in mouse embryonic fibroblasts causes an accumulation of 14-3-3σ, which is responsible for reduced cell proliferation [18]. More recently overexpression of TRIM25 has also been associated with lung and gastric cancers [19,20]. In agreement with these findings, TRIM25 is significantly correlated with poor prognosis in patients with different cancers, especially breast cancer [21].

Walsh et al. uncovered a transcriptional hierarchy underlying breast cancer metastasis using patient-matched primary and metastatic samples, they propose TRIM25 is a master regulator of this hierarchy and promoting metastasis and poor survival, targeting TRIM25 may represent promising future targets for cancer intervention. [22].

We analyzed the sequence of the _TRIM25_ gene and found that pri-miR-3614 is located in the TRIM25 3′-UTR and shares the same promoter. Using the miRNA target prediction software, TargetScan, we found the miR-3614-3p and the miR-3614-5p binding sites at the 3′-UTR of TRIM25, which could likely be occupied to impair host gene transcription or translation. As TRIM25 is aberrantly overexpressed in various types of cancer, including breast cancer (BC), we speculated that there may be an unknown mechanism that can protect TRIM25 mRNA from degradation by miR-3614. Next, we used the starBase website to predict the RBP binding sites on TRIM25 mRNA and found that IGF2BP3 can bind to the TRIM25 3′-UTR at a site proximal to and partially overlapping the miR-3614-3p binding site. Thus, we hypothesized that IGF2BP3 can bind to the TRIM25 3′-UTR and block the maturation of miR-3614, thereby preventing miR-3614-mediated translational repression in BC cells.

2. Materials and methods

2.1. Human tissue specimens and cells

Formaldehyde-fixed paraffin-embedded (FFPE) BC tissues and unpaired mammary hyperplasia (non-tumor tissues) were randomly collected from patients who had undergone surgery at the Shaanxi Provincial People's Hospital in China. Clinicopathological data such as age and gender, as well as histological data, tumor size, lymph node metastasis status, ER status, PR status, and AR status were obtained by reviewing their pathology records. Specimens were collected after obtaining written informed consent from the patients as well as approval of the ethical committees. Patient anonymity was maintained throughout the study. Human BC cell lines MCF-7, HCC1937, MDA-MB-231 and MDA-MB-435, human breast epithelium cells HBL-100 [23] and human embryonic kidney (HEK) 293T cells were obtained from the Cell Bank (Shanghai Institute of Biochemistry and Cell Biology, CAS, Shanghai, China).Cells were maintained in Dulbecco's modified Eagle's medium (DMEM) supplemented with 10% fetal bovine serum (Biological Industries) and 1% antibiotics (100 U/mL penicillin and 100 mg/mL streptomycin sulfate). Cells were grown in 5% CO_2 at 37 °C. The cell line was tested for mycoplasma contamination using the Mycoplasma Detection Kit (Beyotime, Haimen, China) and was found to be negative.

2.2. Plasmid construction and transfection

Human miR-3614 precursor (pre-miR-3614) was synthesized by Shanghai Sangon Biological Engineering Technology and Services Co. Ltd. (Shanghai, China). The pre-miR-3614 coding region was cloned into the pcDNA™6.2-GW/EmGFP (Invitrogen). We constructed pcDNA™6.2-GW/EmGFP-pre-miR-3614. The miR-3614 mimics, anti-miR-3614, small interfering RNAs (siRNAs) and their respective negative control RNAs were purchased from Gima (Shanghai, China). The information of all the sequences are provided in Supplementary Table 2. Transfection was performed using Polyplus transfection kit (Jetprime, France) according to the manufacturer's instructions.

2.3. Lentivirus infection

The plasmid shRNA-IGF2BP3 (sc-60846-SH) was purchased from Santa Cruz Biotechnology. The packaged lentivirus of pre-miR-3614 and si-IGF2BP3 were constructed by GeneChem (Shanghai, China) and named LV-miR-3614 and LV-si-IGF2BP3, respectively. The scramble lentiviral vector LV-Ctrl (or LV-si-Ctrl) was used as a control. The lentiviral vector is expressed green fluorescent protein (GFP) tag. For

infection, the MCF-7 and MDA-MB-231 cells were seeded in a 6-well plate and infected with 1 ml of viral stock containing 5 μg/ml polybrene for 12 h, then this medium was replaced by normal culture medium.

2.4. qRT-PCR

The MCF-7 and MDA-MB-231 cells were plated in 6-well plates at a density of 1.5×10^5 cells per well. The next day, these cells were transfected with siRNAs, plasmids, or control scrambler RNA. Untransfected cells were used as controls. After transfection of 24 h, total cellular RNA was extracted with TRIzol (Invitrogen Carlsbad, USA) according to the manufacturer's protocol. The FFPE tissue samples (10 sections) were deparaffinized by incubating in xylene for 10 min and in 100% ethanol for 5 min, and washed with distilled water for 30 s, followed by RNA extraction using the Qiagen FFPE RNeasy Kit (Valencia, CA, USA) according to manufacturer's instructions. The RNA was quantified with a NanoDrop spectrophotometer (Thermo, USA). The PrimeScript RT Reagent Kit (Takara, Japan) and the SYBR Premix Ex Taq II Kit (Takara, Japan) were used to detect the expression of mature miRNAs and mRNA. The primers used are listed in Table 2. qRT-PCR was performed using an IQ5 Multicolor qRT-PCR Detection System (Bio-Rad, USA). β-actin and U6 expression were used as a control to quantify mRNA and miRNA expression, respectively. The $2^{-\Delta\Delta Ct}$ method was used for the qRT-PCR analysis.

2.5. Western blot

Total protein was harvested from BC cells using RIPA buffer (CST, Boston, China) after 48 h of transfection, and 20–30 μg of protein lysate was separated by 10% SDS-PAGE and transferred to a PVDF membrane (Millipore, USA). The membranes were probed with the following primary antibodies: TRIM25 (1:2000, Abcam, MA, USA), IGF2BP3(1:1000, Abcam), CyclinD1 (1:1000, Cell Signaling Technology, Danvers, MA), CDK4 (11,000, Cell Signaling) for overnight. After washing with TBST buffer, the membrane was incubated with horseradish peroxidase (HRP)-conjugated secondary antibody for 1 h at room temperature. Next, the membranes were incubated with ECL (Pierce, Rockford, IL, USA) for chemiluminescence detection.

2.6. Immunohistochemistry (IHC)

IHC was performed as described previously [24]. Tissue sections (4 μm) were deparaffinized with xylene and hydrated using an alcohol gradient. Endogenous peroxidase-blocking and antigen retrieval were performed sequentially. The sections were incubated with polyclonal rabbit anti-TRIM25 (diluted 1:200, Abcam, MA, USA) and anti-IGF2BP3 (diluted 1:200; Abcam, MA, USA) followed by incubation with a secondary antibody IgG (ZSGB-BIO, China). Histological examination was performed using 3,3′-diaminobenzidine kit (DAB, OriGene, China) and hematoxylin. If the proportion of positive cells was >50% in 5 random fields, the specimen was considered to show high TRIM25/IGF2BP3 expression.

2.7. Luciferase reporter assay

The 3'-UTR of human TRIM25 mRNA was constructed with synthetic oligo-nucleotides and cloned in between the Sac I and Xho I sites of the pmirGLO Dual-luciferase miRNA target expression vector (Promega). We constructed pmirGLO-TRIM25 wild-type (WT) and pmirGLO-TRIM25 mutant-type (MUT). 293T cells were seeded into 96-well culture plates (five wells per group). After 24 h, the cells were transfected with the TRIM25-WT or TRIM25-MUT vector along with pre-miR-3614 plasmid or corresponding control pcDNA6.2-GW. The luciferase activity was measured 24 h post-transfection using the Dual-Glo Luciferase Assay System (Promega, Madison, WI, USA) with Renilla (Rluc)

luciferase activity as the reporter gene and firefly luciferase (Luc) as the reference gene.

2.8. RNA immunoprecipitation (RIP) assay

For the RIP assay, the cell lysates were homogenized according to the protocol specified by the Magna RIP™RNA-Binding Protein Immunoprecipitation Kit (MILLIPORE Catalog No. 17-701). MCF-7 and MDA-MB-231 cells were lysed in RIP lysis buffer containing proteinase inhibitors cocktail tablets (Roche, Cat. 04693116001) and RNAse inhibitor (MILLIPORE, Cat. CS203219) and incubated with anti-IGF2BP3- (Merck, Cat. 03-198), or anti-Ago2 (GeneTex, Cat. GTX60370) or IgG-coupled protein beads for 6 h or overnight at 4 °C. After stringently washing the beads with washing buffer, the bound RNA was purified and subjected to RT–PCR assays.

2.9. Biotin pull-down assay

A biotin pull-down assay was performed using the Pierce™ Magnetic RNA-Protein Pull-Down Kit (Thermo Scientific, MA, USA) according to the manufacturer's instructions. Cell lysates were prepared using RIP lysis buffer. The biotin-labeled TRIM25 RNA probes listed in Table S1. These biotin-labeled probes were bound to streptavidin magnetic beads and incubated for 30 min at room temperature with agitation. A total of 100 μg of isolated protein lysate was added to the RNA-bound beads and incubated for 60 min at 4 °C with agitation. The bound proteins in the pulled-down material were analyzed by Western blot experiments using monoclonal antibodies recognizing IGF2BP3. After secondary antibody incubations, signals were visualized by enhanced chemiluminescence. The RNA probes sequences are listed in Table 2.

2.10. MTT and colony formation

A total of 3×10^3 BC cells was seeded on 96-well plates and cultured (37 °C, 5% CO_2) in DMEM for 12 h. Next, the cells were treated with E2 (100 nM), TAM (100 nM), plasmids (0.1 μg) or siRNA (1.5 pmol) for the MTT cell proliferation assay. Absorbance was measured at a wavelength of 490 nm in a FLUO star OPTIMA microplate spectrophotometer (BMG LABTECH, Offenburg, Germany). Moreover, BC cells (1000 cells) were infected with LV-miR-3614, LV-si-IGF2BP3 and control virus and plated in 6-well plates for colony formation. The cells were grown for 14 days, fixed and stained with crystal violet; colonies with >30 cells were scored.

2.11. Cell cycle assay

BC cells were seeded into 12-well plates at the density of 1×10^6 cells per well. 48 h after transfection, cells were collected by trypsinization, washed with PBS and fixed in ice-cold 70% ethanol at 4 °C overnight. Next, the cells were then washed with PBS and incubated with 0.1 mg/mL RNase A for 15 min and 0.05 mg/mL propidium iodide for 30 min at 4 °C. The samples were sorted based on DNA content by using fluorescence activated cell sorting and CellQuest software (FACScalibur; Becton Dickinson) to determine the percentages of cells that were in the G0/G1, S and G2/M-phases of the cell cycle.

2.12. Xenograft assay

We generated BC cells stably overexpressing miR-3614 or with silenced IGF2BP3 and injected them subcutaneously into female nude mice ($n = 3$/group) of 4–6 weeks of age for tumor engraftment. Tumors were examined every 3 d for a total of 35 d. The tumor volume was calculated using the following formula: $V = lw^2/2$. The growth curves were plotted using the mean of the tumor volumes for each treatment group at a given time point. Five weeks after tumor inoculation mice were killed by cervical dislocation under anesthesia. The tumors were

excised and subjected to analysis. All animal experiments were approved by the Institutional Animal Care and Use Committee of Xi'an Jiaotong University (No. 2017-487) and were performed according to the institution's guidelines for the use of laboratory animals.

2.13. Statistical analysis

All experiments were performed in triplicate at a minimum, unless otherwise stated. Data analyses were carried out using the SPSS 22.0 statistics package (IBM, Armonk, NY, USA). Independent sample Student's t-test and ANOVA analysis were used if the quantitative data between groups show normal distribution. If not consistent with the normal distribution, using the Wilcoxon-Mann-Whitney test. The relationship between TRIM25/miR-3614/IGF2BP3 expression level and clinical parameters was calculated by the χ^2-test. Data are presented as the mean $\pm$ SEM. P values of <0.05 were considered to indicate statistical significance.

3. Results

3.1. Coordinated expression of pri-miR-3614 and its host gene TRIM25 in breast cancer

By conducting The Cancer Genome Atlas (TCGA) database search, we determined that TRIM25 mRNA expression is markedly increased in breast tumor tissues ($P < 0.01$, $n = 389$) compared to that in hyperplastic (non-tumor) tissues ($n = 61$) (Fig. S1a). Next, we quantified the TRIM25 mRNA expression levels in BC samples by qRT-PCR analysis. Consistent with the data from the TCGA analysis, our results indicated that TRIM25 mRNA was upregulated in BC tissues ($n = 30$) compared to that of non-tumor tissues ($P < 0.05$, $n = 30$) (Fig. 1a). We also investigated TRIM25 protein expression levels by

immunohistochemistry. We observed that TRIM25 protein was localized in the nucleus and cytoplasm of BC cells, and found that its expression was upregulated by 83.3% in cancer tissues compared to its expression in hyperplastic tissues (Fig. 1b). Western blot analysis also showed that TRIM25 expression was enriched in BC cell lines compared to the control mammary epithelial cell line, HBL-100 (Fig. 1c). Moreover, the expression of TRIM25 mRNA and protein levels in estrogen-receptor-positive (ER$^+$) BC samples was higher than that of the ER$^-$ BC samples (Fig. 1b and c).

As pri-miR-3614 and its host gene *TRIM25* are both located on chromosome 17q22 and share the same promoter, we suspected that they display similar expression patterns. First, we examined the expression levels of pri-miR-3614 in BC tissues and cell lines by qRT-PCR. In BC and hyperplastic (non-tumor) tissues obtained from 60 BC patients, pri-miR-3614 expression was upregulated (median fold change: 1.5-fold) in 23/30 of the tumor samples, but no significant difference was observed between the ER$^+$ BC and ER$^-$ BC samples (Fig. 1d). This result was further validated in BC cell lines. Pri-miR-3614 expression was higher in the MCF-7 and MDA-MB-231 cancer cell lines compared to the HBL-100 control cell line (Fig. 1e). Next, we examined the levels of mature miR-3614-3p and miR-3614-5p by qRT-PCR. The expression of miR-3614-5p was almost undetectable, likely because miR-3614-3p maturation is prevalent in breast cancer. Unexpectedly, there was no significant difference between the levels of mature miR-3614-3p in BC tissues compared to that of non-tumor tissues, whereas it was found to be significantly lower in BC cell lines (Fig. 1f and g).

To further investigate the roles of TRIM25, pri-miR-3614, and miR-3614-3p expression in BC, clinicopathologic factors were analyzed in relation to their expression levels in BC samples (Table S1). However, the expression of TRIM25, pri-miR-3614 and miR-3614-3p was not associated with lymph node metastasis, ER, PR (progestrone receptor), AR (androgen receptor), p53, E-cadherin, Cerb-2, or Ki67 expression.
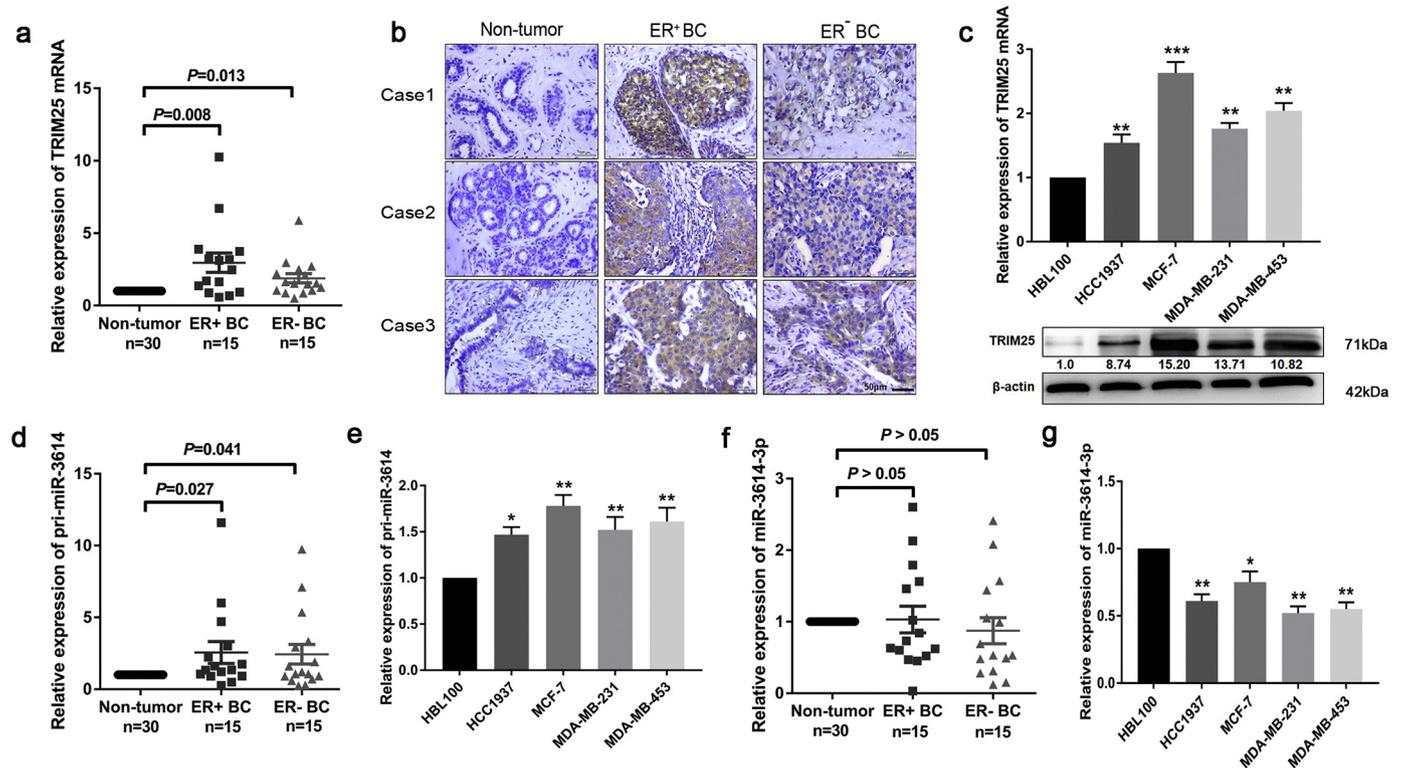

Fig. 1. Endogenous expression of TRIM25, pri-miR-3614, and miR-3614–3p in breast cancer (BC) tissues and BC-derived cell lines. (a) qRT-PCR was performed to examine TRIM25 mRNA expression in BC tissues versus non-tumor tissues. Data are shown as mean $\pm$ SEM (Student's t-test). (b) Representative IHC images of TRIM25 expression in non-tumor tissues and BC tissues. Magnification ×40. Scale bar, 50 μm. (c) TRIM25 mRNA and protein levels in BC cell lines (MCF-7, MDA-MB-231, HCC-1937 and MDA-MB-453) and normal human mammary gland cell line (HBL-100) were quantified by qRT-PCR and Western blot. (d, e) Pri-miR-3614 expression in BC tissues and cell lines. Data are shown as mean $\pm$ SEM (**$P < 0.01$, Student's t-test). (f, g) miR-3614-3p expression in BC tissues and cell lines. Data are presented as the mean $\pm$ SEM. (*$P < 0.05$, **$P < 0.01$, ***$P < 0.001$, Student's t-test).

Altogether, these results indicate that pri-miR-3614 and its host gene TRIM25 exhibit high levels of coordinated expression in BC, with the exception of mature miR-3614-3p.

3.2. E2 promotes the expression of TRIM25 and pri-miR-3614, but does not enhance the formation of miR-3614-3p

Estrogens can promote breast cancer progression by increasing the transcription of proto-oncogenes and growth factors [25]. TRIM25 can act as a primary response gene to mediate estrogen-regulated functions including cellular growth in human breast cancer [26]. Therefore, we hypothesized that miR-3614 transcription may be similarly regulated by estrogen. To test this hypothesis, we treated the ER-positive MCF-7 BC cells and the ERα-negative MDA-MB-231 BC cells with 0–100 nM of estrogen (E2) for 6 h [27,28], and analyzed the levels of TRIM25, pri-miR-3614, and miR-3614-3p using qRT-PCR and western blot. As expected, we observed a significant up-regulation of TRIM25 and pri-miR-3614 expression in MCF-7 cells following the E2 (100 nM) treatment. Similarly, E2 produced the same effect on TRIM25 and pri-miR-3614 expression in MDA-MB-231 cells. However, the levels of miR-3614-3p decreased in both BC cell lines following the E2 treatment (Fig. 2a–d). Subsequently, we demonstrated that estrogen-induced gene expression was completely attenuated by an estrogen antagonist tamoxifen (TAM) in both BC cell lines (Fig. 2e–h).

These data suggest that pri-miR-3614 and its host gene TRIM25 are simultaneously induced by E2 in MCF-7 and MDA-MB-231 cells, which is partially dependent on the estrogen receptor. Pri-miR-3614

transcription in BC is driven by its host gene. However, miR-3614-3p did not occur simultaneously with TRIM25 transcription. Thus, there appears to be a mechanism that suppresses its maturation.

3.3. IGF2BP3 protected TRIM25 by antagonizing miR-3614 decay on TRIM25 mRNA

Next, we investigated the mechanism underlying the inhibition of miR-3614 maturation. Upon analyzing the TRIM25 mRNA sequence, we identified putative RBP binding sites, including HuR- and IGF2BP3-binding motifs. Importantly, there are two binding sites for IGF2BP3 on the TRIM25 gene that are located within the pri-miR-3614 sequence (Fig. 3a). We also analyzed the TCGA data bank and found that the IGF2BP3 level was higher in BC tissues compared to that of non-tumor tissues ($P < 0.01$, $n = 1645$), and identified a significant positive correlation between IGF2BP3 and TRIM25 expression (Fig. S1b and c). Next, we investigated whether IGF2BP3 participates in TRIM25-mediated post-transcriptional regulation of miR-3614. As shown in Fig. 3b–e, siRNA-mediated depletion of IGF2BP3 in MCF-7 and MDA-MB-231 cells reduced the levels of IGF2BP3 and TRIM25 mRNA to 30% and ~50–70%, respectively. A similar trend was observed for pri-miR-3614, but these differences were not statistically significant, whereas the miR-3614-3p levels increased by ~1.5–2-fold compared to that of the scrambled controls. Western blot experiments confirmed that E2 treatment and IGF2BP3 silencing competitively regulated TRIM25 expression (Fig. 3f). We used actinomycin D to inhibit transcription and measure the decay rate of TRIM25 and found that TRIM25 mRNA has a shorter half-life in IGF2BP3-depleted cells relative to control cells
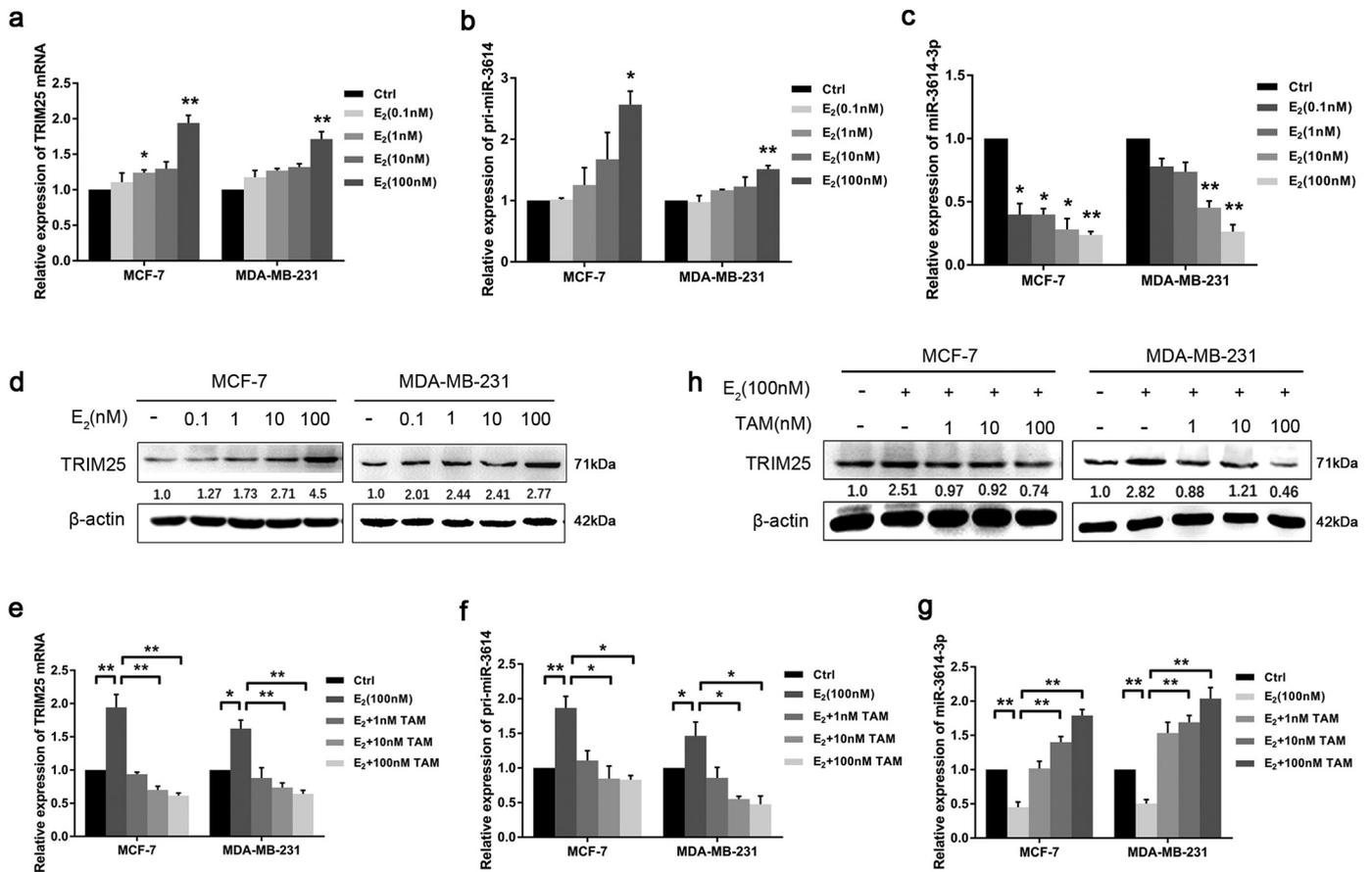

Fig. 2. The expression of TRIM25, pri-miR-3614 and miR-3614-3p in response to estrogen (E2) and tamoxifen (TAM) treatment. (a–c) qRT–PCR analyses of TRIM25 mRNA, pri-miR-3614, and miR-3614-3p expression in MCF-7 and MDA-MB-231 cells treated with the indicated concentrations of E2 (0.1–100 nM) for 6 h. Data are shown as mean ± SEM (*P< 0.05, **P< 0.01, Student's t-test) (d) Western blot analyses of TRIM25 protein level in MCF-7 and MDA-MB-231 cells treated with E2 (0.1–100 nM). (e-g) qRT–PCR analyses of TRIM25 mRNA, pri-miR-3614 and miR-3614-3p levels in BC cells treated with E2 (100 nM) and the indicated concentrations of TAM (1–100 nM). Data are presented as the mean ± SEM. *P< 0.05, **P< 0.01 (Student's t-test). (h) Western blot analyses of TRIM25 protein level in BC cells treated with E2 (100 nM) and TAM (1–100 nM) for 6 h.
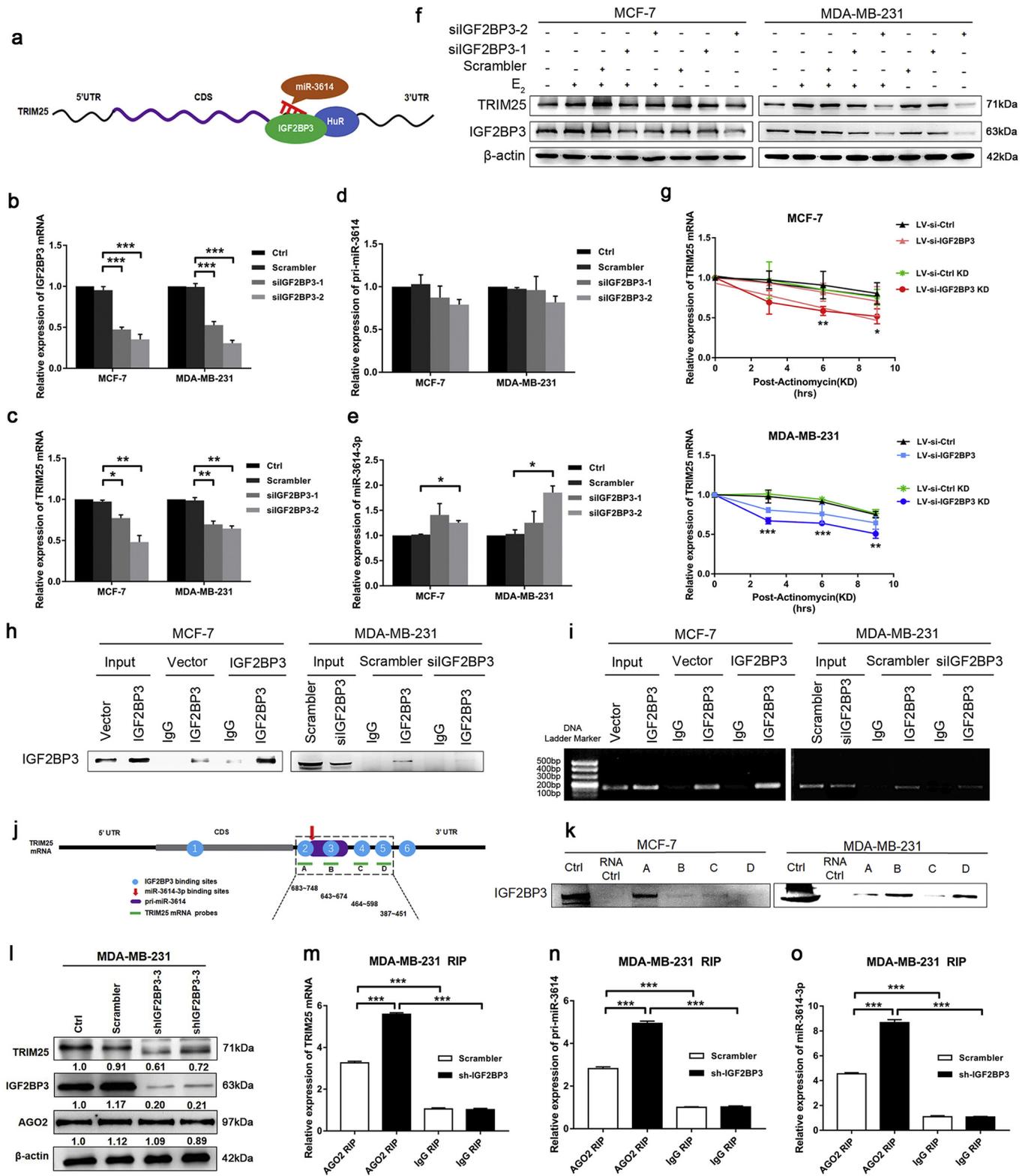
Fig. 3. IGF2BP3 binds to TRIM25 mRNA and inhibits miR-3614 maturation in BC cells. (a) Proposed model of IGF2BP3, HuR and miR-3614 binding sites at the TRIM25 mRNA 3′-UTR. (b–e) The levels of IGF2BP3 mRNA, TRIM25 mRNA, pri-miR-3614 and miR-3614-3p were determined by qRT–PCR after BC cells transfection with si-IGF2BP3 and related controls. Data are presented as the mean ± SEM. (*$P < 0.05$, **$P < 0.01$, ***$P < 0.001$, ANOVA analysis). (f) Forty-eight hours after transfection with si-IGF2BP3 and treatment with E2 (100 nM), the levels of TRIM25, IGF2BP3, and β-actin (loading control) were assessed by Western blot analysis. (g) qRT–PCR analysis of TRIM25 mRNA stability in control or IGF2BP3-depleted BC cells. Data are presented as the mean ± SEM. (*$P < 0.05$, **$P < 0.01$, ***$P < 0.001$, Student's t-test) (h, i) RNA immunoprecipitation (RIP) combined with qRT–PCR assays of IGF2BP3 binding to TRIM25 mRNA in BC cells. Nonspecific rabbit IgG was used as a negative control. Input was used as a positive control. Western blot analysis of IGF2BP3 immunoprecipitated from control or IGF2BP3-overexpressed in MCF-7 cells or IGF2BP3-depleted in MDA-MB-231 cells (H). RT–PCR analysis of RNA precipitated with IGF2BP3 antibody or control IgG (I). (j) Schematic depiction of the TRIM25 (A-D) biotinylated probes used for biotin pull-down analysis. (k) IGF2BP3 in the biotin pull-down samples was detected by Western blot analysis. (l) Western blot of TRIM25 and AGO2 expression in control or IGF2BP3-depleted (sh-IGF2BP3) MDA-MB-231 cells. (m-o) qRT–PCR analysis of RNA precipitated with a-Ago2 (Ago2 RIP) or nonspecific rabbit IgG (IgG RIP). Relative quantification for TRIM25 and IGF2BP2 transcript was performed using β-actin mRNA as a reference gene. Relative quantification for pri-miR-3614 and miR-3614-3p were performed using U6 as a reference gene. Statistical significance was estimated for each comparison using an unpaired t-test (***$P < 0.001$).

(Fig. 3g). However, silencing of HuR did not affect the expression of TRIM25 (Fig. S2). These results indicate that IGF2BP3 can promote TRIM25 expression and suppress miR-3614 maturation.

To confirm the predicted binding sites, we performed RBP immunoprecipitation (RIP) and biotin pull-down analysis. As shown in Fig. 3h and i, TRIM25 mRNA was enriched in IGF2BP3 IP samples compared to the IgG IP samples, suggesting that IGF2BP3 specifically binds to TRIM25 mRNA. Furthermore, we prepared biotinylated probes (~50-nt fragments) spanning the 3′-UTRs at a site proximal and even overlapping the miR-3614-3p binding site, and examined their association with IGF2BP3 using biotin pull-down analysis. Biotinylated TRIM25 RNAs probes were incubated with the cell lysates, and the RBPs from the biotin pull-down were detected by western blot. The results indicate that IGF2BP3 binds to four regions with different affinities. Among them, IGF2BP3 was found to bind preferentially to region A in MCF-7 cells, and to regions B and D in MDA-MB-231 cells (Fig. 3j and k).

Together, these results suggest that IGF2BP3 suppresses the formation of mature miR-3614, thereby protecting TRIM25 mRNA stability.

3.4. IGF2BP3 modulates the interaction of miR-3614 and TRIM25 transcript associated with RISC

These data presented above suggest that IGF2BP3 may attenuate miR-3614-mediated TRIM25 mRNA decay. To further determine if IGF2BP3 protect TRIM25 transcript is associated with RISC, we tested this hypothesis by RIP with Ago2, a RISC component, from control or IGF2BP3-depleted MDA-MB-231 cells and further quantified co-purified RNA by qRT-PCR. Western blot showed IGF2BP3 depletion significantly repressed TRIM25 expression, however unaffected Ago2 expression (Fig. 3l). As expected, RIP showed both of TRIM25 mRNA, pri-miR-3614 and miR-3614-3p co-precipitated with Ago2 from both control and knockdown cells, and enriched concertation with Ago2 increased in IGF2BP3-depleted cells (Fig. 3m–o). The data suggest that IGF2BP3 stabilized TRIM25 mRNA associated with RISC.

3.5. TRIM25 is a direct target of miR-3614-3p in breast cancer

We used Targetscan and RegRNA prediction programs to identify putative miR-3614-3p binding sites in the TRIM25 transcript and found potential miR-3614-3p binding motif which is in the 3′-UTR region. To validate the theoretical relationship between miR-3614-3p and TRIM25, we constructed luciferase reporters by cloning the wild-type 3′-UTRs of TRIM25 (TRIM25-WT) or its mutant version (TRIM25-MUT) into the pmiRGLO dual-luciferase reporter vector (Fig. 4a). Pre-miR-3614-overexpressed plasmid and TRIM25-WT- or MUT-3′-UTR vectors were co-transfected into HEK293T cells. We found that pre-miR-3614 significantly reduced luciferase activity in TRIM25-WT samples but did not significantly affect the TRIM25-MUT samples (Fig. 4b), indicating that miR-3614-3p binds directly to the 3′-UTR of TRIM25.

To further confirm that TRIM25 expression is regulated by miR-3614-3p, we generated MCF-7 and MDA-MB-231 cell lines stably expressing miR-3614 (LV-miR-3614) or transiently transfected with a pre-miR-3614 plasmid, which exhibits a high expression level of miR-3614 compared to that of the control. TRIM25 expression was significantly lower in the miR-3614-overexpressed cell lines (Figs. S3 and S4). Conversely, transfection of a miR-3614-3p inhibitor recovered TRIM25 expression (Fig. 4c and d). Moreover, when the BC cells were co-treated with E2 and pre-miR-3614, the E2-induced expression of TRIM25 was attenuated. When the BC cells were co-treated with E2 and a miR-3614-3p inhibitor, a synergistic effect was observed, similar to that of miR-3614 and siIGF2BP3 co-transfection (Fig. 4e–g). Consistently, IHC staining demonstrated that TRIM25 protein expression was significantly reduced in BC tumors from miR-3614-treated mice compared to the control samples, whereas IGF2BP3 levels remained unaltered (Fig. 4h). Overall, these results indicate that TRIM25 is not only a

host gene, but also a target gene of miR-3614-3p, and that IGF2BP3 competes with the miR-3614 binding sites within the 3′-UTR of TRIM25 mRNA and prevents miR-3614-mediated translation silencing.

3.6. The functions of the TRIM25-miR-3614-3p-IGF2BP3 regulatory axis in BC

Previous studies have shown that E2-induced upregulation of TRIM25 expression significantly promotes BC cell proliferation [29]. As expected, knock-down of TRIM25 in BC cells markedly decreased cell viability and colony formation (Fig. 5a–d), and led to a decrease in number of cells in the G1 phase, owing to the decreased levels of Cyclin D1 and CDK4 (Fig. 5e and f). These data suggested that TRIM25 can act as oncogene to promote BC cell proliferation and G1-S cell cycle transition via regulation of Cyclin D1 and CDK4.

Meanwhile, the overexpression of miR-3614 inhibited E2-induced TRIM25 expression at both the mRNA and protein levels (Fig. 3c and d), and impaired cell growth and colony formation, whereas miR-3614–3p inhibitor moderately increased BC cell growth, perhaps due to the low expression levels of miR-3614-3p in MCF-7 and MDA-MB-231 cells (Fig. 6a and b). Moreover, the overexpression of miR-3614 led to an accumulation of BC cells in the G1-phase compared to the negative control, and induced G1-phase arrest via Cyclin D1 and CDK4 signaling pathways. However, the inhibition of miR-3614-3p promoted the transition from the G1 to the S phase (Fig. 6c and d). Additionally, xenograft assays showed that tumor nodules derived from miR-3614-overexpressing cells grew slower than the control cells. The average volume of the miR-3614-treated tumors was markedly less than that of the controls (Fig. 6e). These results demonstrate that miR-3614-3p inhibits cell growth by inducing cell cycle arrest in BC cells, and may act as a tumor suppressor in BC. The overexpression of miR-3614 caused a similar effect on BC cell growth with silencing of TRIM25.

We further examined the functional effect of IGF2BP3 on BC cells. First, we assessed the level of IGF2BP3 in BC tissues and non-tumorous tissues by qRT-PCR and IHC. As shown in Fig. S5A and B, significantly higher levels of IGF2BP3 were observed in BC tissues compared to that of non-tumor tissues ($p < 0.05$, $n = 30$). Next, we used lentivirus to generate IGF2BP3-depleted cell lines (LV-si-IGF2BP3). The expression levels of IGF2BP3 and TRIM25 were markedly reduced in the IGF2BP3-depleted cells (Fig. S6). Moreover, IGF2BP3 silencing inhibited growth and colony formation in MCF-7 and MDA-MB-231 cells (Fig. 7a and b). In vivo, xenografts infected with LV-si-IGF2BP3 grew slower than the controls (Fig. 7c). We also found that BC tumors with IGF2BP3-depleted cells expressed less TRIM25 at the protein level (Fig. 7d). Importantly, co-treatment with miR-3614-3p mimics, siIGF2BP3, and TAM synergized to markedly reduce the proliferation of BC cells (Fig. 7e). Collectively, these findings indicate that the TRIM25-miR-3614-IGF2BP3 axis plays an important role in regulating the growth of BC cells.

4. Discussion

Multiple examples of cooperative and competitive interplay between RBPs and miRNAs in the regulation of gene expression have been previously described [30–33]. In this study, we identified a novel mechanism of mRNA translational regulation mediated by an antagonistic interplay between a microRNA and an RBP. We found that intragenic miR-3614 inhibits the expression of its host gene *TRIM25* by binding to its 3′-UTR, and that IGF2BP3 can competitively occupy this binding site to inhibit miR-3614 maturation, thereby protecting TRIM25 mRNA from miR-3614-mediated degradation.

TRIM25, also known as estrogen-responsive finger protein, is upregulated in response to estrogen. The TRIM25 mRNA was expressed in human breast tumors and the estrogen-induced expression of the TRIM25 was found in MCF-7 human breast cancer cells. Moreover, TRIM25 promoter activity was enhanced through the estrogen-
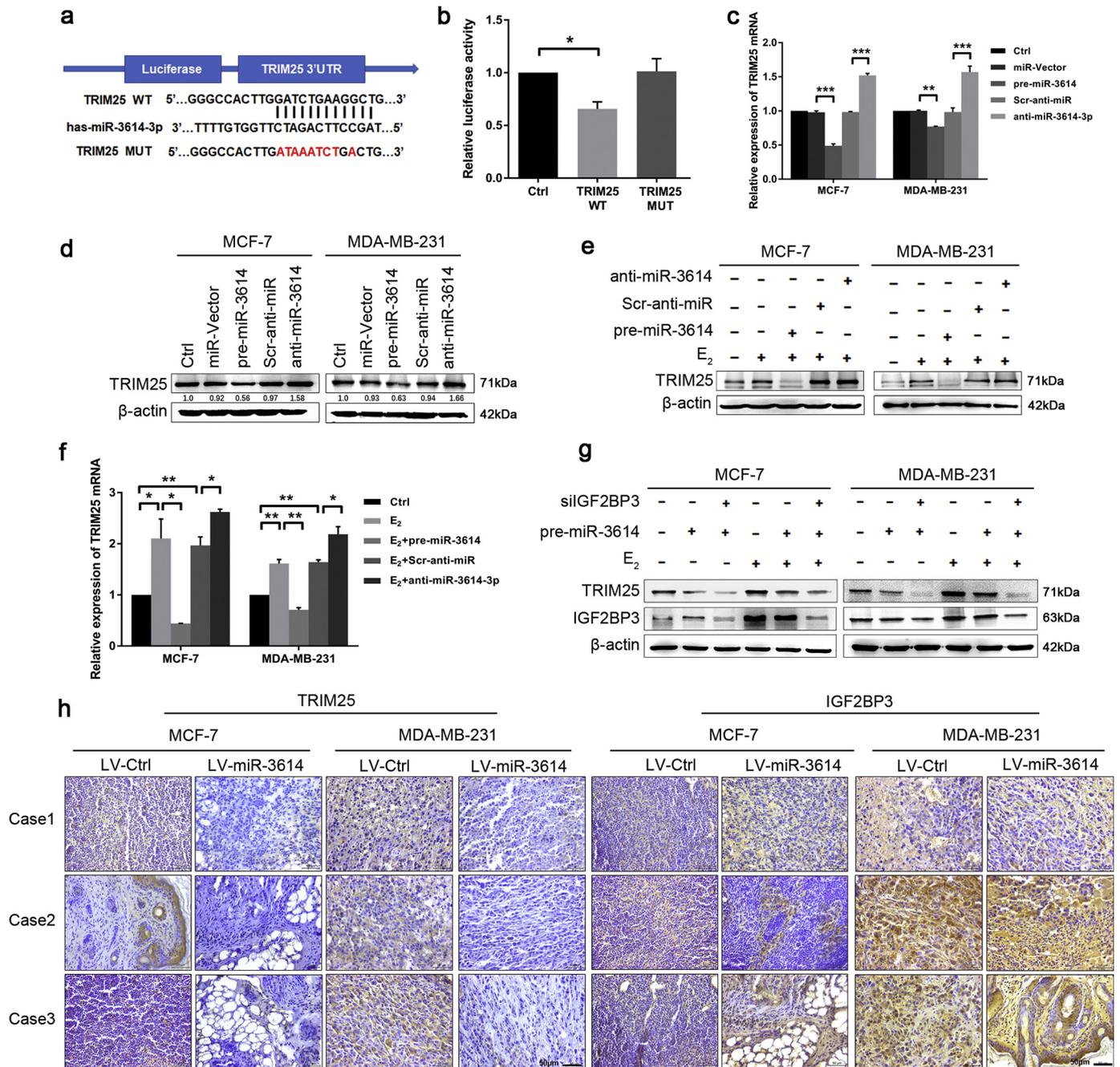
Fig. 4. The host gene TRIM25 is a direct target of miR-3614-3p. (a) miR-3614-3p binding sites within the 3′-UTR of TRIM25. (b) Dual-luciferase reporter assays showing repression of the wild-type TRIM25 3′-UTR by miR-3614-3p in HEK293T cells. Data are shown as mean ± SEM (*P < 0.05, Student's t-test) (c, d) The expression of TRIM25 was assayed by qRT-PCR and Western blot after overexpression of pre-miR-3614 by transfection with pre-miR-3614-pcDNATM6.2-GW/EmGFP or inhibition of pre-miR-3614 by transfection with antisense oligonucleotides of miR-3614 (anti-miR-3614) in MCF-7 and MDA-MB-231 cells. Data are presented as the mean ± SEM. (**P < 0.01, ***P < 0.001, ANOVA analysis). (e, f) qRT-PCR and Western blot experiments were performed to measure the TRIM25 expression in BC cells treated with pre-miR-3614/anti-miR-3614-3p plus E2 or related negative controls. Data are shown as mean ± SEM (*P < 0.05, **P < 0.01, Student's t-test). (g) Western blot analysis of protein expression of TRIM25 and IGF2BP3 in BC cells after co-transfection with siIGF2BP3, pre-miR-3614-3p, and E2. (h) IHC staining of TRIM25 (left) and IGF2BP3 (right) in tumor tissues from mice implanted with LV-miR-3614 or LV-Ctrl BC cells. Magnification ×40. Scale bar, 50 μm.

responsive element dependent on estrogen and estrogen receptor [34]. Previously, Ikeda et al. showed TRIM25 mRNA expression in 9 of 15 (60.0%) breast carcinoma tissues by using RNase protection assay, and Takashi et al. reported TRIM25 immunoreactivity in breast carcinoma cells in 22 of 30 (73.3%) cases which was significantly associated with an increased risk of recurrence and adverse clinical outcome of the patients [21,29]. In this study, we observed that TRIM25 was upregulated in BC tissues and cell lines, consistent with previous literature. We showed a coordinated and strong expression of pri-miR-3614 and its host gene *TRIM25*; however, mature miR-3614-3p was significantly downregulated in BC cells. Furthermore, treatment with E2 significantly increased pri-miR-3614 and TRIM25 expression in both MCF-7 and MDA-MB-231 cells, consistent with the results that TRIM25 expression can be regulated by factors independent of estrogen or estrogen signaling [22]. In contrast, the expression of mature miR-3614-3p was significantly decreased, and TAM blocked the effects of the estrogen-mediated induction. There has a common consensus MDA-MB-231 is a triple-negative breast carcinomas (TNBC) cell line, that lack ERα but express low levels of ERβ [35]. In our other study, we found that MDA-MB-231 cell also express EGFR (data not shown) which is
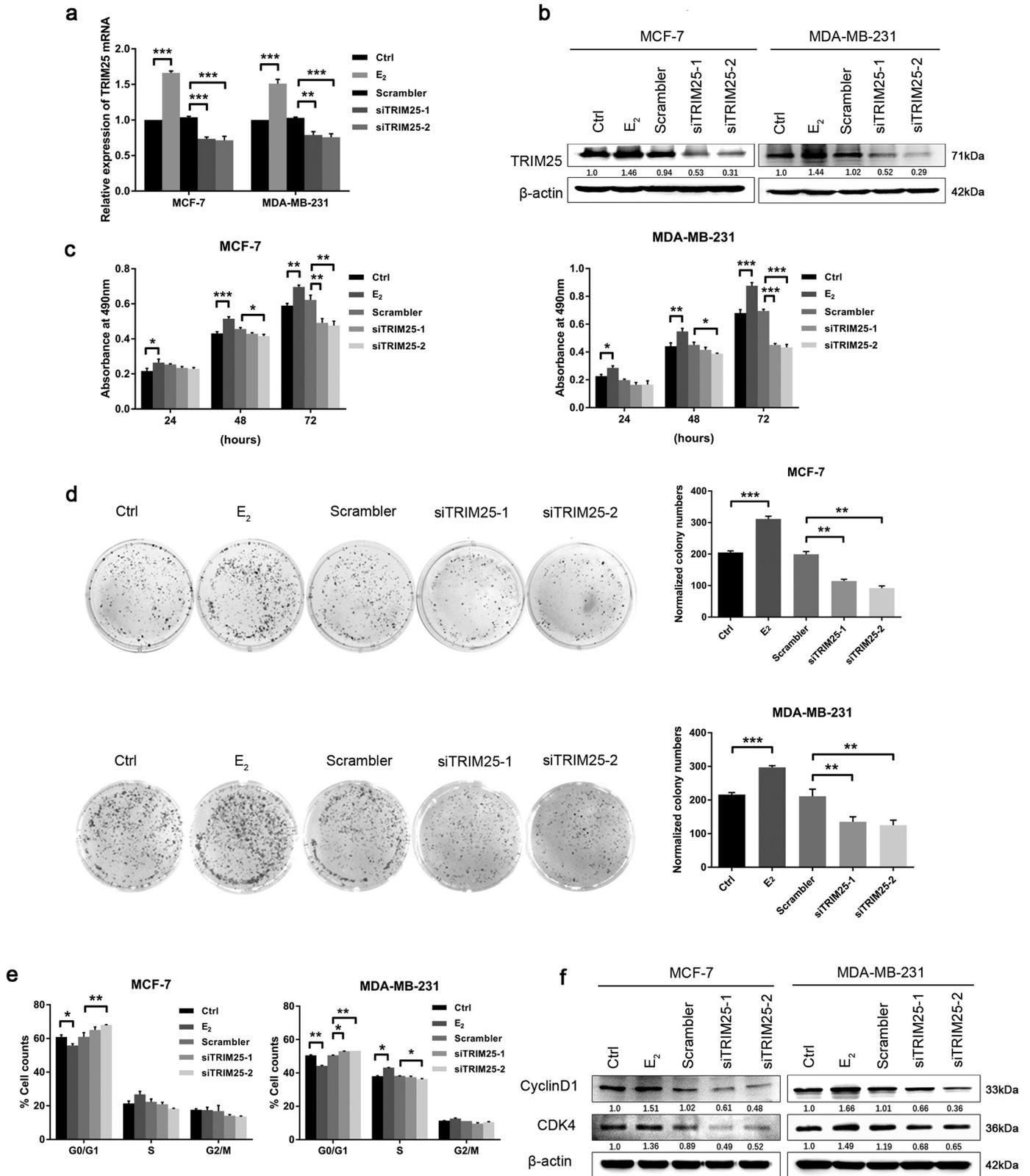
Fig. 5. TRIM25-depleted interferes with E2-dependent BC cell proliferation. (a, b) qRT–PCR and Western blot were performed to detect the expression level of TRIM25 in MCF-7 and MDA-MB-231 cells after transfection with E2, si-TRIM25, or scrambler RNA. Data are presented as the mean $\pm$ SEM. (**$P < 0.01$, ***$P < 0.001$, ANOVA analysis). (c, d) The effects of TRIM25 expression on BC cell proliferation was determined by using the MTT assay and colony formation analysis. The absorbance of the plates was read on a microplate reader at a wavelength of 490 nm. Data are presented as the mean $\pm$ SEM. (*$P < 0.05$, **$P < 0.01$, ***$P < 0.001$, ANOVA analysis). (e) The cell cycle distribution was analyzed by flow cytometry after transfection with E2, si-TRIM25, or scrambler RNA. The histogram indicates the percentage of cells in the G0/G1, S, and G2/M cell cycle phases. The representative results are presented as the mean $\pm$ SD. Each experiment was repeated at least three times, and each sample was assayed in triplicate. (*$P < 0.05$, **$P < 0.01$, ANOVA analysis) (f) The expression of CDK4, CyclinD1, and β-actin analyzed by Western blot after transfection with E2, si-TRIM25, or scrambler RNA.
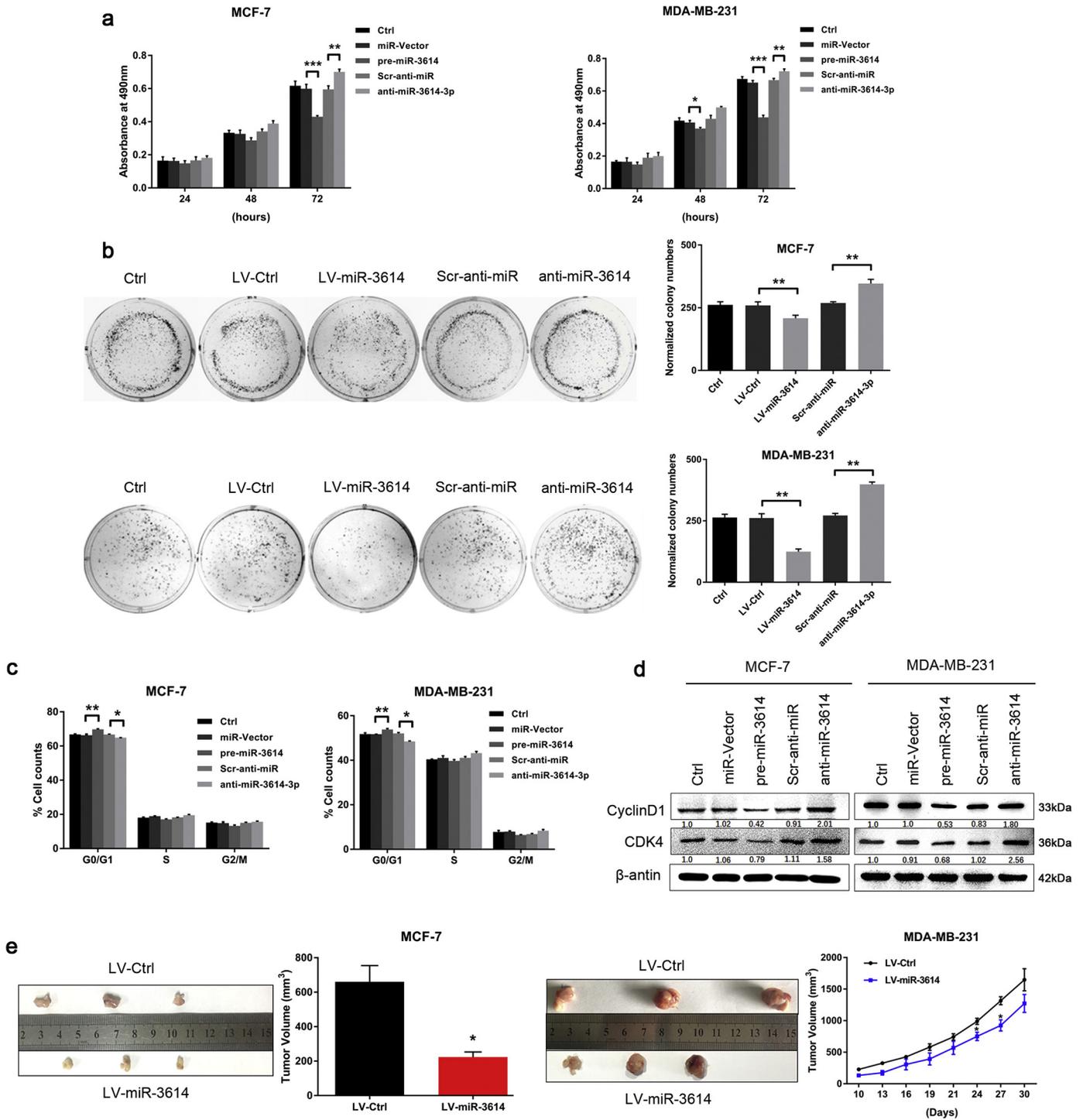
Fig. 6. MiR-3614-3p suppresses BC cell proliferation. (a, b) MTT cell proliferation assay and colony formation were performed at the indicated time points after transfection with pre-miR-3614, anti-miR-3614, or negative control. Data are presented as the mean ± SEM. (*P < 0.05, **P < 0.01, ***P < 0.001, ANOVA analysis). (c) miR-3614-3p increases G1 phase arrest in BC cells. Flow cytometry analysis of BC cells transfected with pre-miR-3614, anti-miR-3614, or negative control treatment. Data are presented as the mean ± SEM. (*P < 0.05, **P < 0.01, ANOVA analysis). (d) The expression of CDK4, CyclinD1, and β-actin analyzed by Western blot after transfection with pre-miR-3614, anti-miR-3614, or negative control. (e) Xenograft studies show suppressed tumor growth when pre-miR-3614 is overexpressed in the transplanted cells. Gross morphology of tumors after 30 days of implantation with either LV-miR-3614 or LV-Ctrl cells (n = 3) (left). Tumor growth curves of the tumor volumes represent measurement taken every 3 d for 30 d (right). Data are shown as mean ± SEM (*P < 0.05, Student's t-test).

consistent with Samanta S′ report. Therefore, MDA-MB-231 cells cannot be considered completely triple-negative cell. In addition, estrogen not only activate the classical estrogen receptor, also can be act to RTKs and G protein-coupled estrogen receptor 1 (GPER), through the activation of PI3K/AKT signaling pathways induced the expression of target genes [36,37]. The effects of estrogens binding to these classical estrogen receptors are delayed. However, estrogens binding to GPER lead

to a fast effect on regulation of gene transcription. GPER is positive in MDA-MB-231 cell. Therefore, these may be the reason why E2 treatment MDA-MB-231 cell also increased the expression of TRIM25 and pri-miR-3614.

Thus, an important question was raised: What causes such a discrepancy between host gene *TRIM25* and mature miR-3614-3p transcript levels in BC cells? Upon examining the TRIM25 mRNA sequence, we
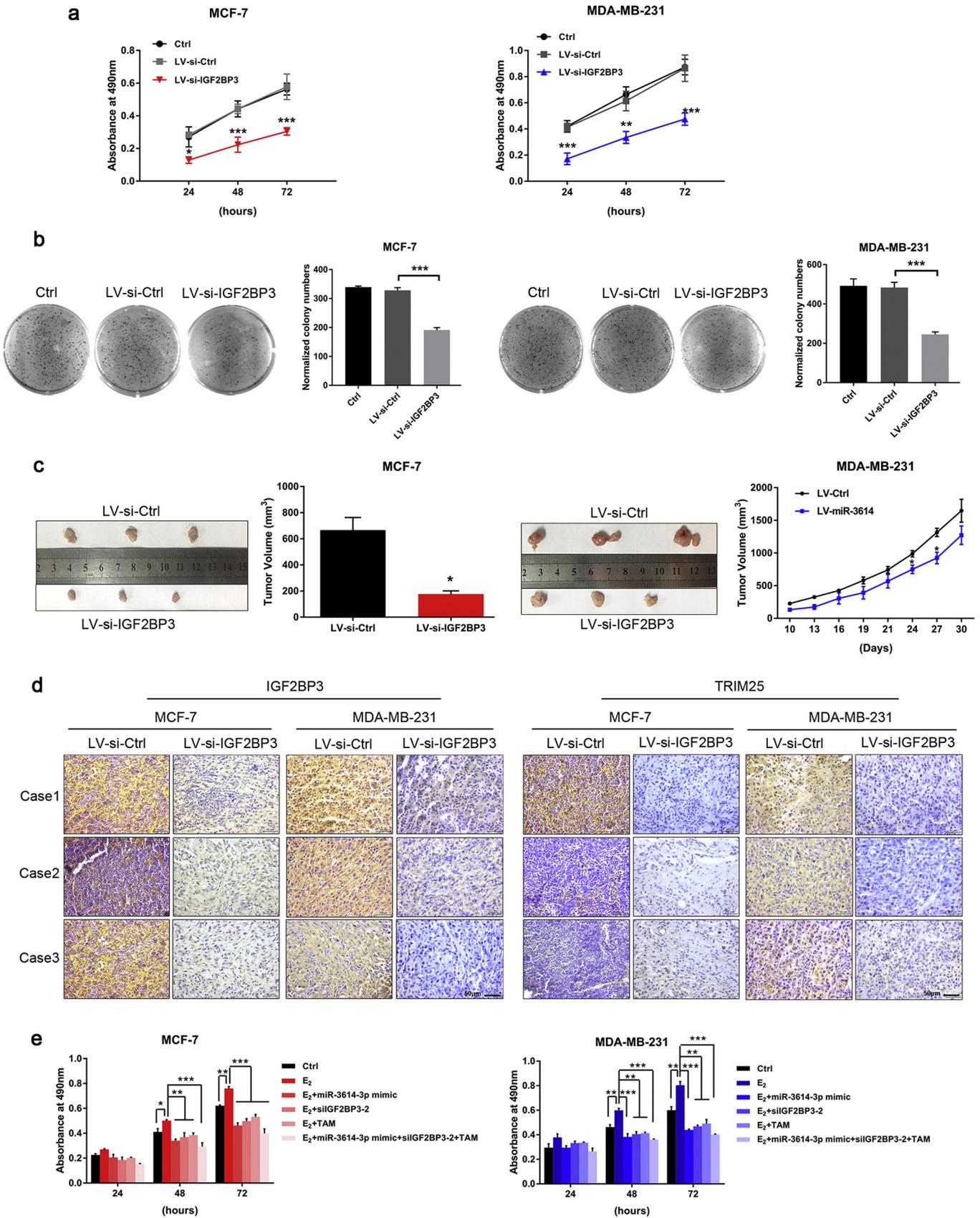
Fig. 7. IGF2BP3-depleted inhibits BC cell proliferation. (a, b) MTT assay and colony formation were performed at the indicated time points after transfection with LV-si-IGF2BP3 or related control. Data are presented as the mean ± SEM. *P < 0.05, **P < 0.01 (Student's t-test and ANOVA analysis). (c) Xenograft experiments showing suppressed tumor growth in response to IGF2BP3 knock-down. Gross morphology of tumors after 30 days of injection of either MCF-7/MDA-MB-231-LV-si-IGF2BP3 or MCF-7/MDA-MB-231-LV-si-Ctrl cells (n = 3) (left). Tumor growth curves of the tumor volumes represent measurements taken every 3 d for 30 d (right). Data are shown as mean ± SEM (*P < 0.05, Student's t-test). (d) IHC staining of TRIM25 (right) and IGF2BP3 (left) in tumor tissues from mice implanted with MCF-7/MDA-MB-231-LV-si-IGF2BP3 or MCF-7/MDA-MB-231-LV-si-Ctrl cells. Magnification ×40. Scale bar, 50 μm. (e) MTT assay of BC cells after co-treatment with miR-3614-3p, si-IGF2BP3, TAM, and E2. Data are presented as the mean ± SEM. *P < 0.05, **P < 0.01 (Student's t-test).
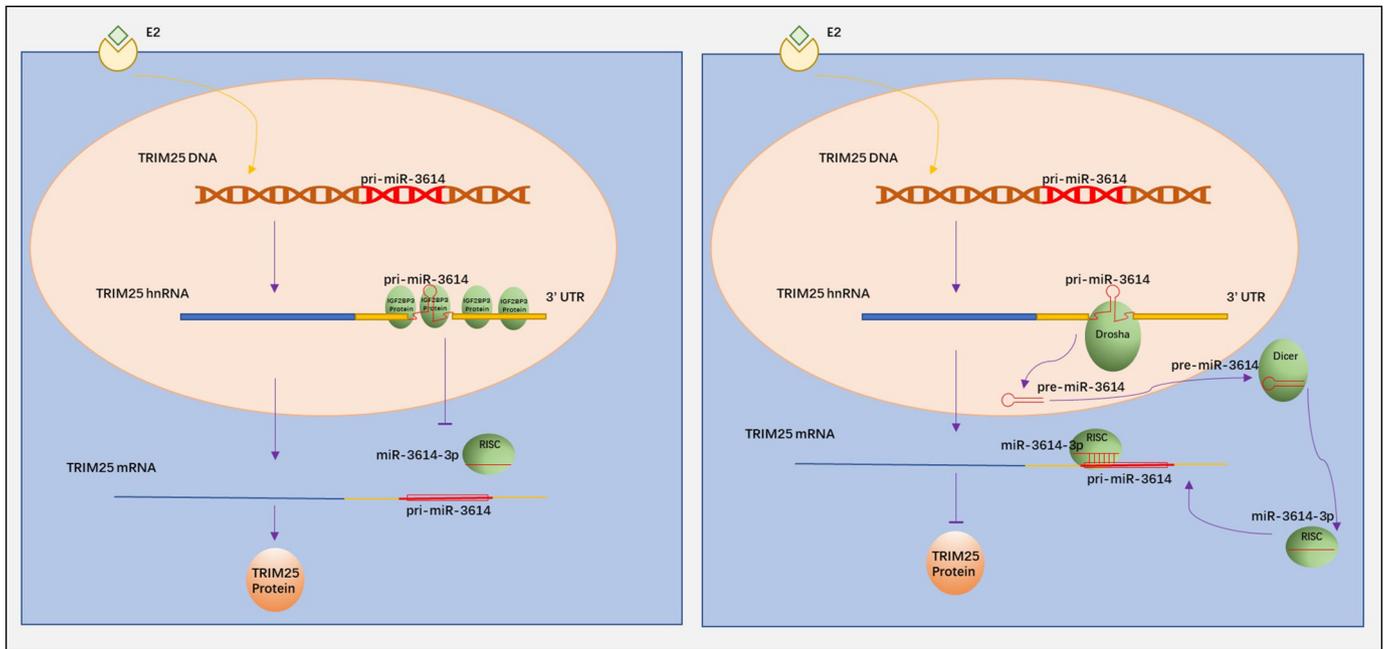
Fig. 8. Proposed mechanism of IGF2BP3- and miR-3614-mediated regulation of TRIM25 expression by binding to the 3′-UTR of TRIM25. (a) IGF2BP3 binds to the 3′-UTR of TRIM25, blocks miR-3614 maturation and protects TRIM25 mRNA by preventing miR-3614-3p binding to the 3′-UTR. (b) Depletion of IGF2BP3 results in increased expression of miR-3614-3p that binds to the 3′-UTR of TRIM25, leading to translational repression of TRIM25.

identified putative RBP binding sites, including IGF2BP3-binding motifs. Hanane et al. identified 164 direct mRNA targets of IGF2BP3 in pancreatic ductal adenocarcinoma cells using iCLIP and RIP analysis. IGF2BP3 may attenuate miRNA-mediated mRNA degradation in association with Ago2 [8]. In this study, we confirmed that TRIM25 is a target gene of IGF2BP3. Using actinomycin D to interrupt TRIM25 transcription, we determined that IGF2BP3 prolonged the half-life of TRIM25. RIP and Pull-down analysis indicated that IGF2BP3 binds to the 3′-UTR of the TRIM25 stabilized transcript, and blocks the pri-miR-3614 processing. Next, we checked binding level of pre-miR-3614 and TRIM25 upon silencing of IGF2BP3 by RIP with Ago2, a RISC component. The results suggest IGF2BP3 stabilized TRIM25 mRNA associated with RISC. Thus, here we identified a new mechanism whereby IGF2BP3 influences the miRNA-mRNA interaction by modulating miRNA maturation.

Furthermore, we found that TRIM25 is not only a host gene, but also a target gene of miR-3614 in BC. The overexpression of miR-3614 significantly inhibited the expression of TRIM25 by binding to pri-miR-3614 at the 3′-UTR of TRIM25, suggesting that miR-3614-3p may suppress *TRIM25* expression. Moreover, the IGF2BP3-binding sites overlap with the miR-3614-3p-binding site, revealing that IGF2BP3 can inhibit the binding of miR-3614-3p to its target. Thus, IGF2BP3 and miR-3614 compete for common binding sites within the 3′-UTR of TRIM25, thereby regulating its translation.

Previous studies have demonstrated that TRIM25 and IGF2BP3 play an essential role in cancer cell proliferation [38]. For example, TRIM25 is a potent regulator of metastatic disease and associated with poor survival outcomes for breast cancer [22,39]. TRIM25 also acts as an oncogene in colorectal cancer and it activates TGF-β signaling pathway to promote tumor proliferation and metastasis [40]. Besides, IGF2BP3 protein is variably expressed in mantle cell lymphoma and that strong expression in a high percentage of tumor cells is tightly associated with an increased proliferation capacity of the tumor cells. In breast carcinomas, a significantly upregulated expression of IGF2BP3 was found in adenoid cystic carcinomas [41] and a novel biomarker for triple-negative invasive mammary carcinoma associated with a more aggressive phenotype [42,43]. In this study, the results demonstrate that the expression patterns and functions of TRIM25/IGF2BP3 and miR-3614-3p in BC are quite different. TRIM25 and IGF2BP3 promotes

cell proliferation and functions as a tumor oncogene in cancer cells. However, miR-3614-3p inhibits BC cell growth, thus acting as a tumor suppressor. In vivo, both the silencing of IGF2BP3 and the overexpression of miR-3614 can effectively inhibit the growth of BC tumors in xenograft models. Interestingly, co-treatment with siIGF2BP3, TAM, and miR-3614-3p effectively reduced TRIM25 expression and inhibited the proliferation of BC cells, indicating a synergistic effect.

Based on our observations, we propose a model for the regulation of TRIM25 mRNA translation in which IGF2BP3 and miR-3614-3p can competitively bind to the 3′-UTR of TRIM25 mRNA. IGF2BP3 protects TRIM25 mRNA from degradation and suppresses miR-3614 maturation in BC (Fig. 8A and B). Moreover, the tumor-promoting role of TRIM25 in breast cancer was exerted through its regulation of cell cycle by interaction with IGF2BP3 and miR-3614-3p. Altogether, the IGF2BP3–TRIM25–miR-3614 axis functions represent a new pathway that regulates tumor cell proliferation, thereby providing a rationale for targeting IGF2BP3 and TRIM25 in breast cancer treatment.

Funding sources

Conflicts of interest

The authors declare no conflicts of interest.

Authors' contributions

C.H., Y.K.C. and A.L. conceived and supervised the project. Z.Z.W., Y.K.C., D.D.T., C.H. and Z.H.Z designed and performed most of the experiments. X.F·W and Q.L conducted bioinformatic and biostatistical

analyses. L.C, T.J. and X.Y.L. acquired the patient data and assisted in the in vivo tumor model experiments. Z.Z.W, Y.K.C wrote the paper.

Data sharing

Supplementary data to this article can be found online at DOI: http://dx.doi.org/10.17632/y9bvs8kz56.1#file-01010d05-b8ae-46cd-8403-8c9fc197b108.

Appendix A. Supplementary data

Supplementary data to this article can be found online at https://doi.org/10.1016/j.ebiom.2018.12.061.

References

[1] Zealy RW, Wrenn SP, Davila S, Min KW, Yoon JH. microRNA-binding proteins: specificity and function. Wiley Interdiscip Rev RNA 2017;8.
[2] Treiber T, Treiber N, Plessmann U, Harlander S, Daiss JL, Eichner N, et al. A compendium of RNA-binding proteins that regulate microRNA biogenesis. Mol Cell 2017;66 (270-284 e13).
[3] Gerstberger S, Hafner M, Tuschl T. A census of human RNA-binding proteins. Nat Rev Genet 2014;15:829–45.
[4] Blackinton JG, Keene JD. Post-transcriptional RNA regulons affecting cell cycle and proliferation. Semin Cell Dev Biol 2014;34:44–54.
[5] Vanderweyde T, Youmans K, Liu-Yesucevitz L, Wolozin B. Role of stress granules and RNA-binding proteins in neurodegeneration: a mini-review. Gerontology 2013;59: 524–33.
[6] Bell JL, Wachter K, Muhleck B, Pazaitis N, Kohn M, Lederer M, et al. Insulin-like growth factor 2 mRNA-binding proteins (IGF2BPs): post-transcriptional drivers of cancer progression? Cell Mol Life Sci 2013;70:2657–75.
[7] Leontieva OV, Ionov Y. RNA-binding motif protein 35A is a novel tumor suppressor for colorectal cancer. Cell Cycle 2009;8:490–7.
[8] Ennajdaoui H, Howard JM, Sterne-Weiler T, Jahanbani F, Coyne DJ, Uren PJ, et al. IGF2BP3 modulates the interaction of invasion-associated transcripts with RISC. Cell Rep 2016;15:1876–83.
[9] Lee Y, Ahn C, Han J, Choi H, Kim J, Yim J, et al. The nuclear RNase III Drosha initiates microRNA processing. Nature 2003;425:415–9.
[10] Lund E, Guttinger S, Calado A, Dahlberg JE, Kutay U. Nuclear export of microRNA precursors. Science 2004;303:95–8.
[11] Bartel DP. MicroRNAs: genomics, biogenesis, mechanism, and function. Cell 2004; 116:281–97.
[12] Ying SY, Lin SL. Intron-derived microRNAs–fine tuning of gene functions. Gene 2004; 342:25–8.
[13] Hinske LC, Galante PA, Kuo WP, Ohno-Machado L. A potential role for intragenic miRNAs on their hosts' interactome. BMC Genomics 2010;11:533.
[14] Jonson L, Christiansen J, Hansen TV, Vikesa J, Yamamoto Y, Nielsen FC. IMP3 RNP safe houses prevent miRNA-directed HMGA2 mRNA decay in cancer and development. Cell Rep 2014;7:539–51.
[15] Vikesaa J, Hansen TV, Jonson L, Borup R, Wewer UM, Christiansen J, et al. RNA-binding IMPs promote cell adhesion and invadopodia formation. EMBO J 2006;25: 1456–68.
[16] Choudhury NR, Heikel G, Trubitsyna M, Kubik P, Nowak JS, Webb S, et al. RNA-binding activity of TRIM25 is mediated by its PRY/SPRY domain and is required for ubiquitination. BMC Biol 2017;15:105.
[17] Gack MU, Shin YC, Joo CH, Urano T, Liang C, Sun L, et al. TRIM25 RING-finger E3 ubiquitin ligase is essential for RIG-I-mediated antiviral activity. Nature 2007;446: 916–20.
[18] Urano T, Saito T, Tsukui T, Fujita M, Hosoi T, Muramatsu M, et al. Efp targets 14-3-3 sigma for proteolysis and promotes breast tumour growth. Nature 2002;417:871–5.
[19] Zhu Z, Wang Y, Zhang C, Yu S, Zhu Q, Hou K, et al. TRIM25 blockade by RNA interference inhibited migration and invasion of gastric cancer cells through TGF-beta signaling. Sci Rep 2016;6:19070.
[20] Qin Y, Cui H, Zhang H. Overexpression of TRIM25 in lung cancer regulates tumor cell progression. Technol Cancer Res Treat 2016;15:707–15.
[21] Suzuki T, Urano T, Tsukui T, Horie-Inoue K, Moriya T, Ishida T, et al. Estrogen-responsive finger protein as a new potential biomarker for breast cancer. Clin Cancer Res 2005;11:6148–54.
[22] Walsh LA, Alvarez MJ, Sabio EY, Reyngold M, Makarov V, Mukherjee S, et al. An integrated systems biology approach identifies TRIM25 as a key determinant of breast cancer metastasis. Cell Rep 2017;20:1623–40.
[23] Pussinen PJ, Karten B, Wintersperger A, Reicher H, McLean M, Malle E, et al. The human breast carcinoma cell line HBL-100 acquires exogenous cholesterol from high-density lipoprotein via CLA-1 (CD-36 and LIMPII analogous 1)-mediated selective cholesteryl ester uptake. Biochem J 2000;349:559–66.
[24] Sun R, Liu Z, Wang L, Lv W, Liu J, Ding C, et al. Overexpression of stathmin is resistant to paclitaxel treatment in patients with non-small cell lung cancer. Tumour Biol 2015;36:7195–204.
[25] Dickson RB, Lippman ME. Estrogenic regulation of growth and polypeptide growth factor secretion in human breast carcinoma. Endocr Rev 1987;8:29–43.
[26] Horie K, Urano T, Ikeda K, Inoue S. Estrogen-responsive RING finger protein controls breast cancer growth. J Steroid Biochem Mol Biol 2003;85:101–4.
[27] Dickson RB, Huff KK, Spencer EM, Lippman ME. Induction of epidermal growth factor-related polypeptides by 17 beta-estradiol in MCF-7 human breast cancer cells. Endocrinology 1986;118:138–42.
[28] Falany JL, Macrina N, Falany CN. Regulation of MCF-7 breast cancer cell growth by beta-estradiol sulfation. Breast Cancer Res Treat 2002;74:167–76.
[29] Ikeda K, Orimo A, Higashi Y, Muramatsu M, Inoue S. Efp as a primary estrogen-responsive gene in human breast cancer. FEBS Lett 2000;472:9–13.
[30] Kedde M, Agami R. Interplay between microRNAs and RNA-binding proteins determines developmental processes. Cell Cycle 2008;7:899–903.
[31] Ciafre SA, Galardi S. microRNAs and RNA-binding proteins: a complex network of interactions and reciprocal regulations in cancer. RNA Biol 2013;10:935–42.
[32] Hao J, Duan FF, Wang Y. MicroRNAs and RNA binding protein regulators of microRNAs in the control of pluripotency and reprogramming. Curr Opin Genet Dev 2017;46:95–103.
[33] Wang F, Song W, Zhao H, Ma Y, Li Y, Zhai D, et al. The RNA-binding protein QKI5 regulates primary miR-124-1 processing via a distal RNA motif during erythropoiesis. Cell Res 2017;27:416–39.
[34] Hatakeyama S. TRIM proteins and cancer. Nat Rev Cancer 2011;11:792–804.
[35] Samanta S, Sharma VM, Khan A, Mercurio AM. Regulation of IMP3 by EGFR signaling and repression by ERbeta: implications for triple-negative breast cancer. Oncogene 2012;31:4689–97.
[36] Revankar CM, Cimino DF, Sklar LA, Arterburn JB, Prossnitz ER. A transmembrane intracellular estrogen receptor mediates rapid cell signaling. Science 2005;307: 1625–30.
[37] Sakamoto H, Matsuda K, Hosokawa K, Nishi M, Morris JF, Prossnitz ER, et al. Expression of G protein-coupled receptor-30, a G protein-coupled membrane estrogen receptor, in oxytocin neurons of the rat paraventricular and supraoptic nuclei. Endocrinology 2007;148:5842–50.
[38] Meyerson NR, Zhou L, Guo YR, Zhao C, Tao YJ, Krug RM, et al. Nuclear TRIM25 specifically targets influenza virus ribonucleoproteins to block the onset of RNA chain elongation. Cell Host Microbe 2017;22 (627–638 e7).
[39] Ito K, Suzuki T, Akahira J, Sakuma M, Saitou S, Okamoto S, et al. 14-3-3sigma in endometrial cancer–a possible prognostic marker in early-stage cancer. Clin Cancer Res 2005;11:7384–91.
[40] Sun N, Xue Y, Dai T, Li X, Zheng N. Tripartite motif containing 25 promotes proliferation and invasion of colorectal cancer cells through TGF-beta signaling. Biosci Rep 2017;37.
[41] Vranic S, Gurjeva O, Frkovic-Grazio S, Palazzo J, Tawfik O, Gatalica Z. IMP3, a proposed novel basal phenotype marker, is commonly overexpressed in adenoid cystic carcinomas but not in apocrine carcinomas of the breast. Appl Immunohistochem Mol Morphol 2011;19:413–6.
[42] Walter O, Prasad M, Lu S, Quinlan RM, Edmiston KL, Khan A. IMP3 is a novel biomarker for triple negative invasive mammary carcinoma associated with a more aggressive phenotype. Hum Pathol 2009;40:1528–33.
[43] Bellezza G, Prosperi E, Del Sordo R, Colella R, Rulli A, Sidoni A. IMP3 is strongly expressed in malignant phyllodes tumors of the breast: an immunohistochemical study. Int J Surg Pathol 2016;24:37–42.